



# An Intertropical Convergence Zone shift controlled the terrestrial material supply on the Ninetyeast Ridge

Xudong Xu<sup>1,3,4</sup>, Jianguo Liu<sup>1,2,4</sup>, Yun Huang<sup>1</sup>, Lanlan Zhang<sup>1,4</sup>, Liang Yi<sup>5</sup>, Shengfa Liu<sup>2,6</sup>, Yiping Yang<sup>1,4</sup>, Li Cao<sup>7</sup>, and Long Tan<sup>1,3,4</sup>

<sup>1</sup>Key Laboratory of Ocean and Marginal Sea Geology, South China Sea Institute of Oceanology, Chinese Academy of Sciences, Guangzhou 510301, China

<sup>2</sup>Laboratory for Marine Geology, Pilot National Laboratory for Marine Science and Technology, Qingdao 266061, China

<sup>3</sup>University of Chinese Academy of Science, Beijing 100049, China

<sup>4</sup>Southern Marine Science and Engineering Guangdong Laboratory (Guangzhou), Guangzhou 511458, China

<sup>5</sup>State Key Laboratory of Marine Geology, Tongji University, Shanghai 200092, China

<sup>6</sup>Key Laboratory of Marine Geology and Metallogeny, First Institute of Oceanography, Ministry of Natural Resources, Qingdao 266061, China

<sup>7</sup>Shandong Provincial Research Institute of Coal Geology Planning and Exploration, Jinan 250104, China

**Correspondence:** Jianguo Liu (jgliu@scsio.ac.cn) and Yun Huang (huangyun@scsio.ac.cn)

Received: 24 October 2021 – Discussion started: 18 November 2021

Revised: 15 April 2022 – Accepted: 14 May 2022 – Published: 22 June 2022

**Abstract.** Among various climate drivers, direct evidence for the Intertropical Convergence Zone (ITCZ) control of sediment supply on the millennial scale is lacking, and the changes in ITCZ migration demonstrated in paleoclimate records need to be better investigated. Here, we use clay minerals and Sr–Nd isotopes obtained from a gravity core on the Ninetyeast Ridge to track the corresponding source variations and analyze the relationship between terrestrial material supply and climatic changes. On the glacial–interglacial scale, chemical weathering weakened during the North Atlantic cold-climate periods and falling sea level hindered the transport of smectite into the study area due to the exposure of Andaman and Nicobar Islands. However, the influence of the South Asian monsoon on the sediment supply was not obvious on the millennial scale. We suggest that the north–south migration of the ITCZ controlled the rainfall in Myanmar and further directly determined the supply of clay minerals on the millennium scale because the transport of smectite was highly connected with the ITCZ location; thus, the regional shift of the ITCZ induced an abnormal increase in the smectite percentage during the late Last Glacial Maximum (LGM) in our records. The smectite percentage in the studied core is similar to distinct ITCZ records but different in some periods, revealing that regional changes in the ITCZ were

significantly obvious, the ITCZ is not a simple north–south displacement, and closer connections occurred between the Northern–Southern Hemisphere in the eastern Indian Ocean during the late LGM.

## 1 Introduction

Deposited sediments are essential recorders of the paleoclimate and paleoceanographic conditions since the climate is tied to the whole sedimentation process from weathering and transport to the deposition of sediments on land. The terrestrial materials of “source–sink” systems are supplied to marine environments under the combined effects of multiple climate-related driving forces and ocean processes (Li et al., 2018; Yu et al., 2019), and understanding these effects is crucial for reconstructing the coevolutionary relationship of the paleoenvironment with the paleoceanographic conditions and paleoclimate. Various factors may control the formation and transport of terrestrial materials at low latitudes, such as the northeastern Indian Ocean. Recently, the South Asian monsoon has been revealed to be the main driving force of terrestrial material supply in Bangladesh and of hydrological changes in the Bay of Bengal (BoB, Dutt et al., 2015; Gebre-

giorgis et al., 2016; Joussain et al., 2017; Li et al., 2018; Liu et al., 2021). Moreover, the Intertropical Convergence Zone (ITCZ) is an important climate-driving force in low-latitude regions (Deplazes et al., 2013; Ayliffe et al., 2013), which has a pivotal role in heat transportation on Earth (Schneider et al., 2014), and the north–south shift of the ITCZ is thought to connect the climates in the Northern and Southern Hemisphere (Huang et al., 2019; Zhuravleva et al., 2021). Because monsoon dynamics are shaped by large-scale meridional temperature gradients and an ITCZ shift in tropical monsoon areas (Mohtadi et al., 2016), there are hopeful opportunities to analyze sediment responses to ITCZ or monsoon variations. The paleoclimate breakthroughs mentioned above enable us to analyze the response of sedimentary records to the ITCZ shift in the BoB more accurately. However, evidence for direct control of terrestrial sediment supply by the ITCZ remains lacking, which is an obstacle to understanding the response of the depositional environment to the ITCZ shift.

As the main deposition area for vast amounts of weathered Himalayan materials, the BoB accumulates numerous Himalayan terrestrial materials that are loaded by the Ganges–Brahmaputra (G-B) River (Goodbred and Kuehl, 2000) and forms the largest subaqueous fan, the Bengal Fan (3000 km long from north to south, 1400 km wide from east to west, with an area of  $3.9 \times 10^5$  km<sup>2</sup>; Curray et al., 2003). The eastern and western sides of the BoB correspond to the Andaman Sea and the Indian Peninsula, respectively, and the BoB is a natural site that is useful for studying the interactions between weathering and climatic factors since both sides of the bay are affected by the South Asian monsoon (Ali et al., 2015). Previous studies suggest that Himalayan material transported by the G-B River was the predominant source of material in the northern BoB (Li et al., 2018; Ye et al., 2020), and the main sources in the west BoB are the Indian Peninsula and Himalayan weathered material (Kessarkar et al., 2005; Tripathy et al., 2011, 2014). In the eastern BoB, the sediment source areas include the Himalayan (transported by the G-B river), Indo-Burman ranges, and the Myanmar region through which the Irrawaddy River flows (Colin et al., 1999; Joussain et al., 2016). The terrigenous detrital material in the Andaman Sea is mainly Myanmar-origin sediments transported by the Irrawaddy River (Ali et al., 2015; Awasthi et al., 2014; Colin et al., 2006). A series of terrigenous sediment issues, such as changes in the source area and proportion of terrigenous matter in various regions of the BoB from the LGM to the Holocene, the distribution range of terrigenous materials in the western and eastern BoB, and how the G-B River sediments are transported in the BoB, has been unclear until now. Little attention has been given to sediment provenance in the southern BoB or, particularly, to the correlation of these sediment sources with climatic driving factors.

Recent studies have revealed that clay minerals can be used to effectively track changes in source areas in the source–sink system of the BoB due to the great differences in

clay mineral components among the source areas around the BoB (Joussain et al., 2016; Li et al., 2017; Liu et al., 2019; Ye et al., 2020). Moreover, Sr–Nd isotopes have been widely reported to track the variations in sediment provenance in the BoB (Ahmad et al., 2005; Colin et al., 1999, 2006).

In this study, we measured clay minerals and Sr–Nd isotopes in a deep-sea gravity core obtained from the southeastern BoB (Fig. 1) to reconstruct variations in the sources of sediments in the Ninetyeast Ridge and to further explore the climate forces that affected the supply of terrestrial materials during the past 45 kyr. Core 17I106, located above the abyssal plain at  $\sim 900$  m, is exempt from the influence of large-scale turbidite activities and receives only fine-grained pelagic sediments that can reflect the changes in the provenance of the surrounding source area (Fig. 1), which makes the terrestrial sediments on the Ninetyeast Ridge suitable for exploring the relationship between the paleoclimate and paleoenvironment in the BoB. Here, we aim to disentangle the ITCZ variability signal in marine sediments from multiple driving forces and further understand the response of sedimentary records to ITCZ migrations.

## 2 Materials and methods

### 2.1 Chronology

Gravity core 17I106 (90.0040° E, 6.2105° N, water depth 2928 m) was collected by the R/V *Shiyan 1* vessel belonging to the South China Sea Institute of Oceanology (SCSIO), Chinese Academy of Sciences (CAS) from the Ninetyeast Ridge, northeast of the Indian Ocean (Fig. 1). This core has a total length of 162 cm and consists of gray to green silty clays subsampled at 1 cm intervals. The age model of core 17I106 was reconstructed based on 10 accelerator mass spectrometry (AMS) <sup>14</sup>C dates and Bayesian interpolations between these dates (Fig. 2 and Table 1). AMS <sup>14</sup>C dating was performed on mixed planktonic foraminifera at Beta Analytic Inc. More than 20 mg of intact mixed planktonic foraminifera shells was selected from the  $> 150 \mu\text{m}$  fractions of each sample (10 g dried sample). All radiocarbon ages were converted and reported as calendar years before present with the Calib8.2 software program with the Marine20 calibration dataset (Reimer et al., 2020). A continuous depth–age model was performed using Bacon software by dividing a sedimentary sequence into many thin segments and estimating a linear accumulation rate for each segment based on the calibrated <sup>14</sup>C dates and a Bayesian approach (Blaauw and Christen, 2011).

### 2.2 Clay mineralogy

Clay minerals ( $< 2 \mu\text{m}$ ) were separated from the sediment samples by sedimentation according to Stokes' settling velocity principle after organic materials and carbonates were removed with 15 % hydrogen peroxide (H<sub>2</sub>O<sub>2</sub>) and 0.1 N hy-

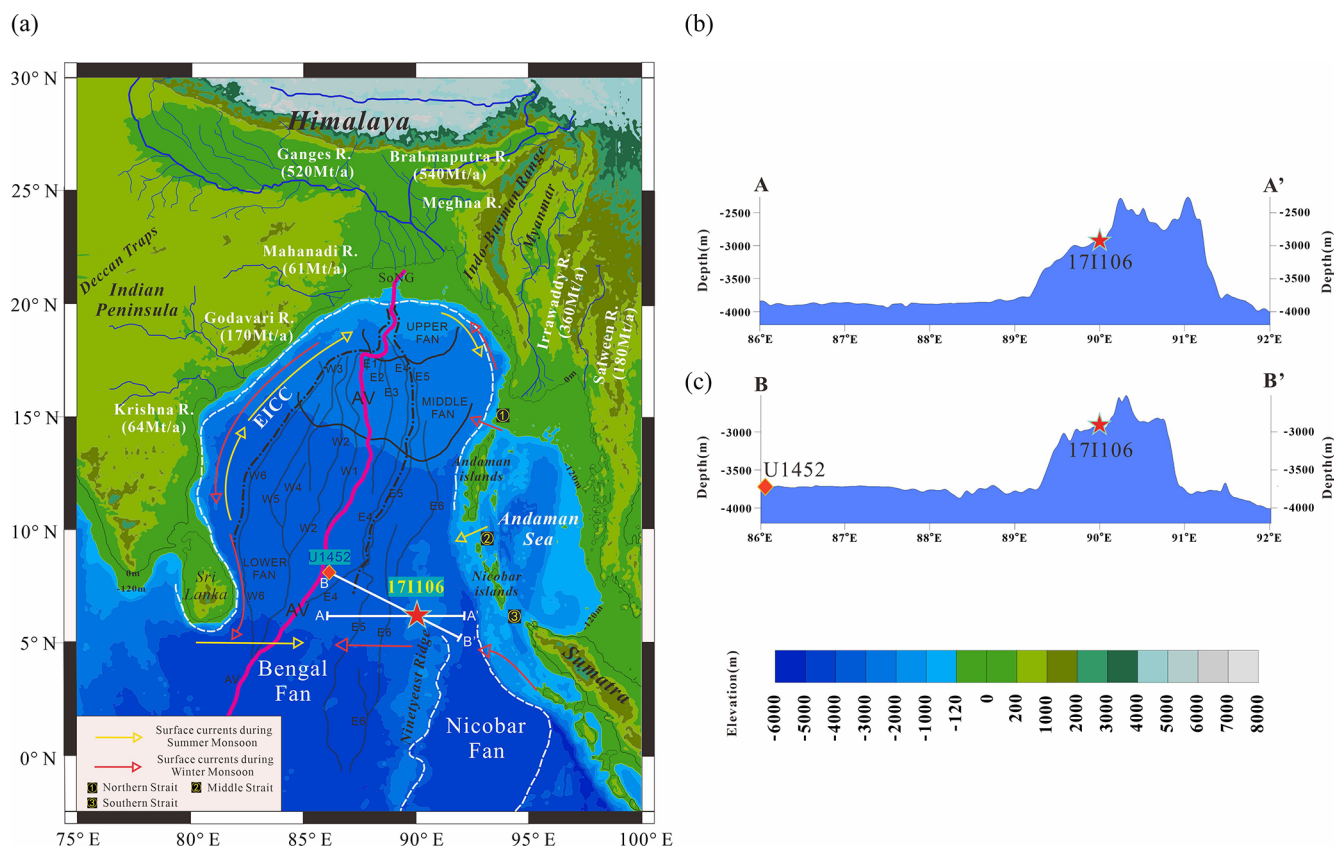


**Figure 1.** Geographical setting of the BoB. The locations of cores 171106 (red asterisks) and U1452 (orange diamond) are shown. (a) The white dashed lines outline the scale of the Bengal Fan and the Nicobar Fan. The pink solid line is the “active” channel, and solid gray lines and black letters represent the turbidity channel and the reference names of the principal channels. The dotted–dashed line is the outline of the most recently active subfan (Curry et al., 2003). (b, c) The solid white lines denote the two profile positions with the elevation legend.

**Table 1.** Carbon-14 and calibrated calendar ages of mixed planktonic foraminifera measured in core 171106 in the northeastern Indian Ocean.

Number	Depth (cm)	Materials	Measured $^{14}\text{C}$ age (years BP, $\pm 1\sigma$ )	Calendar median age (years BP)
1	5	mixed planktonic foraminifera	4160 $\pm$ 30	4053
2	25	mixed planktonic foraminifera	10 690 $\pm$ 40	11 880
3	31	mixed planktonic foraminifera	11 460 $\pm$ 40	12 801
4	58	mixed planktonic foraminifera	17 910 $\pm$ 50	20 710
5	69	mixed planktonic foraminifera	20 050 $\pm$ 60	23 183
6	93	mixed planktonic foraminifera	24 590 $\pm$ 90	27 883
7	101	mixed planktonic foraminifera	27 820 $\pm$ 120	31 074
8	125	mixed planktonic foraminifera	31 820 $\pm$ 200	35 455
9	133	mixed planktonic foraminifera	36 370 $\pm$ 280	40 434
10	157	mixed planktonic foraminifera	42 190 $\pm$ 560	44 167

drochloric acid (HCl), respectively. We used the sedimentation method by placing the sample in glassware with an inner diameter of 7 cm and a height of 10 cm at an experimental temperature of 19 °C. The sedimentation time was calculated as 4 h and 10 min according to Stokes’ formula. The upper 5 cm of liquid was extracted, followed by centrifugation at 4800 rpm for 10 min, and the smear was made into a natu-

ral slice. The natural slice was heated in an oven at 60 °C for 24 h to make ethylene glycol saturated slides for the subsequent test. The clay mineral slides were measured using routine X-ray diffraction (XRD) equipment (Bruker Inc, D8 ADVANCE) in the Key Laboratory of Ocean and Marginal Sea Geology, SCSIO, CAS. Clay mineral abundance was calculated by measuring the peak areas of smectite (15–17 Å),

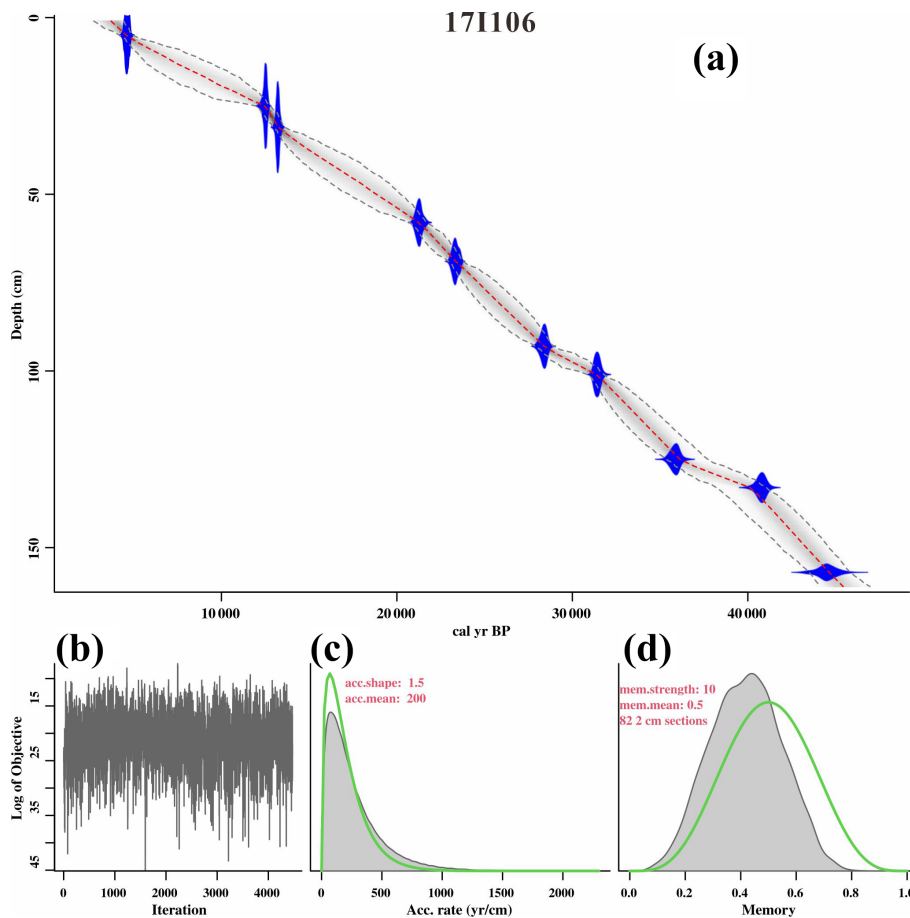


**Figure 2.** Age–depth model of core 171106 in the northeastern Indian Ocean. **(a)** Calibrated  $^{14}\text{C}$  dates (blue, with  $2\sigma$  errors) and the resulting age–depth model (the darker gray shading indicates more likely calendar ages, the gray stippled lines show 95 % confidence intervals, and the red curve shows the single “best” model based on the weighted mean age for each depth). **(b)** Number of Markov chain Monte Carlo (MCMC) iterations used to generate the grayscale graphs. **(c)** Prior (green) and posterior (gray) distributions of the sediment accumulation rates (the mean sediment accumulation rate was  $\sim 2 \text{ yr cm}^{-1}$ ). **(d)** Prior (green) and posterior (gray) memory distributions (dependence of the sediment accumulation rate between neighboring depths).

illite ( $10 \text{ \AA}$ ), and kaolinite–chlorite ( $7 \text{ \AA}$ ). Relative proportions of kaolinite and chlorite were calculated from the ratio of  $3.57 \text{ \AA} / 3.54 \text{ \AA}$  peak areas. The relative percentages of the four main clay minerals were estimated by calculating the integrated peak areas of characteristic basal reflections using Topas5P software with the empirical factors by Biscaye (1965). The reproducibility error of this method is  $\pm 5 \%$ – $10 \%$ .

### 2.3 Sr–Nd isotope analyses

A total of 22 samples ( $< 63 \mu\text{m}$  from core 171106) were selected for isotope analyses, and we used the experimental method described by Dou et al. (2016). Carbonates were removed from 70 to 100 mg powdered bulk samples by leaching with  $0.25 \text{ N HCl}$  for 24 h at  $50 \text{ }^\circ\text{C}$ . The residues were then completely digested in high-pressure Teflon bombs using a  $\text{HCl} + \text{HNO}_3 + \text{HClO}_4 + \text{HF}$  solution. Rb and Sr were

separated in  $2.5 \text{ N HCl}$  using Bio-Rad AG50W-X12 200–400 mesh cation exchange resin. Sm and Nd were separated in  $0.15 \text{ N HCl}$  using P507 cation exchange resin. The strontium (Sr) and neodymium (Nd) isotopic compositions of the sediment samples were measured using a Thermo Scientific multi-collector inductively coupled plasma mass spectrometer (MC-ICPMS Nu plasma) at the Key Lab of Marine Sedimentology and Environmental Geology, Ministry of Natural Resources, China. The organic materials and carbonate were removed from the samples by  $\text{H}_2\text{O}_2$  and  $\text{HCl}$ , respectively. For the convenience of direct comparison, the Nd isotopic ratio results are expressed as  $\epsilon\text{Nd}(0) = [({}^{143}\text{Nd}/{}^{144}\text{Nd})_{\text{meas}}/0.512638 - 1] \times 10000$  using the present CHUR value (Jacobsen and Wasserburg, 1980). Replicate analyses of NBS-987 during the study gave a mean  ${}^{87}\text{Sr}/{}^{86}\text{Sr}$  of  $0.710310 \pm 0.000003$  (2s), which is close to its certified value of 0.710245. Similarly, replicate analyses of

JNDi-1 gave a mean  $^{143}\text{Nd}/^{144}\text{Nd}$  of  $0.512112 \pm 0.000004$  (2s), and its certified value was 0.511860.

### 3 Results

The age model is built based on 10 radiocarbon dates from core 17I106. The top age is 3.8 ka, and the bottom age is 44.9 ka; thus, this core covers a continuous sedimentary succession of the last  $\sim 45000$  years. The sedimentation rates in the Holocene (average  $3.1 \text{ cm ka}^{-1}$ ) were relatively lower than those during the last glacial period (average  $4.6 \text{ cm ka}^{-1}$ ), with the highest rate of  $8.3 \text{ cm ka}^{-1}$  during 12.5–13.6 ka BP (Fig. 3a). In the study core, the illite percentage ranges from 31 % to 63 % with an average of 48 %, while the smectite percentage ranges between 8 % and 57 % with an average of 30 % (Fig. 3b–e). Moreover, the kaolinite percentage ranges from 2 % to 16 %, and the chlorite percentage ranges from 5 % to 20 % in the core sediments. In the study core, the  $^{87}\text{Sr}/^{86}\text{Sr}$  ratios range from 0.7122015 to 0.7186141 with an average of 0.7161698, while  $\epsilon\text{Nd}$  values range from  $-13.02$  to  $-10.29$  with an average of  $-11.24$  (Fig. 3f–g). In this study core, the  $^{87}\text{Sr}/^{86}\text{Sr}$  ratio and  $\epsilon\text{Nd}$  values remain stable before the LGM but show fluctuations after the LGM, without obvious increasing or decreasing tendencies. During  $\sim 14.5$ – $12.5$  ka,  $^{87}\text{Sr}/^{86}\text{Sr}$  ratios significantly increased from 0.7139 to 0.7172, while  $\epsilon\text{Nd}$  values decreased abruptly from  $-10.28$  to  $-13.02$ .

### 4 Discussion

#### 4.1 Sediment provenance and transport patterns

The lower sedimentation rates ( $3$ – $5 \text{ cm ka}^{-1}$ , Fig. 3a) measured in core 17I106 were in accordance with the normal sedimentation rates obtained from neighboring cores around the Ninetyeast Ridge (Ahmad et al., 2005; Raza and Ahmad, 2013). In this region, turbidite activities were less developed (Joussain et al., 2016; Fournier et al., 2017), in accordance with far distance from the active channel (Fig. 1). In the northern BoB, due to heavy river runoff and steep topography, the G-B River system transports a large amount of the products of Himalayan physical denudation; these products mainly consist of illite and chlorite formed under dry and cold-climate conditions (Chamley, 1989; Khan et al., 2019). Because of the hot and humid conditions in Myanmar and the Indian Peninsula, sediments in these regions are formed through the chemical weathering of silicate minerals and thus have high smectite percentages. Moreover, the Irrawaddy River brought weathered products characterized by high smectite percentages from Myanmar into the Andaman Sea, leading to high smectite percentages in the terrestrial sediments deposited in this marine environment (Ali et al., 2015).

The relatively high illite percentages measured in core 17I106 indicate that the weathered Himalayan materials car-

ried by the G-B River system are the primary source of sediments in the study area (Fig. 4a). Compared with the large amounts of materials loaded by the G-B River system, the weathered areas and runoff volumes of the Indo-Burman ranges are relatively small, and consequently, their sediment contributions are limited in the study area, although their sediments are also characterized by relatively high illite percentages (Joussain et al., 2016). Evidence of surface sediments in the BoB further reveals that the smectite percentages of sediments in the central region are significantly lower than those in the eastern and western regions (Li et al., 2017; Liu et al., 2019), indicating that sediments of Indian Peninsula origin are difficult to transport into the eastern BoB through the central BoB. Because the limited weathering area of Andaman and Nicobar Islands cannot provide a large amount of smectite according to provenance studies (Ali et al., 2015), the Myanmar materials characterized by high smectite percentages have the advantage of shorter transport distances compared to those sourced from the Indian Peninsula as the main source area of smectite around the BoB. Therefore, the most important source of smectite in the study area is the Myanmar region. In marine environments, kaolinite is preferentially deposited in estuary areas due to mineral segregation (Gibbs, 1977) and thus may not be transported over long distances, so the kaolinite in the study area was most likely sourced from neighboring Sumatra (Fig. 4a, Liu et al., 2012). The Sr–Nd isotopes measured in the studied core are close to those measured in the Irrawaddy, Indo-Burman ranges, and Sumatra source regions (Fig. 4b), indicating that terrestrial materials with diameters  $< 63 \mu\text{m}$  mainly come from the Irrawaddy River, Indo-Burman ranges, and Sumatra source areas, which was confirmed by an Sr–Nd isotope study in the southwestern part of the study area (Ahmad et al., 2005) and is consistent with sediment provenance studies in the Ninetyeast Ridge on different timescales (Ali et al., 2021; Seo et al., 2022). This difference in clay minerals and isotopes may be consistent with the view that clay minerals may be transported over long distances, while coarser terrestrial sediments can only be transported to more proximate locations.

In the northeastern BoB, the southwest monsoon turns southward into the Andaman Sea, resulting in the transport of sediments from the Indo-Burman Range and Irrawaddy River to the central Andaman Sea (Colin et al., 2006). The location of core 17I106, drilled on the Ninetyeast Ridge, was above the abyssal plain, and the terrestrial materials deposited to the west of this location are difficult to resuspend and deposit on the ridge under the force of bottom currents or turbidity currents. In fact, the G-B-loaded materials are mainly carried eastward by surface ocean currents in summer to the Andaman Sea, where the seasonal surface currents load materials from the Himalayan and Indo-Burman ranges into the Andaman Sea through the northern strait (NS) (P. Liu et al., 2020; Rayaroth et al., 2016). These G-B River sediments can also be transported southward along the west side of the Andaman and Nicobar Islands (Fig. 5), and a westward ocean

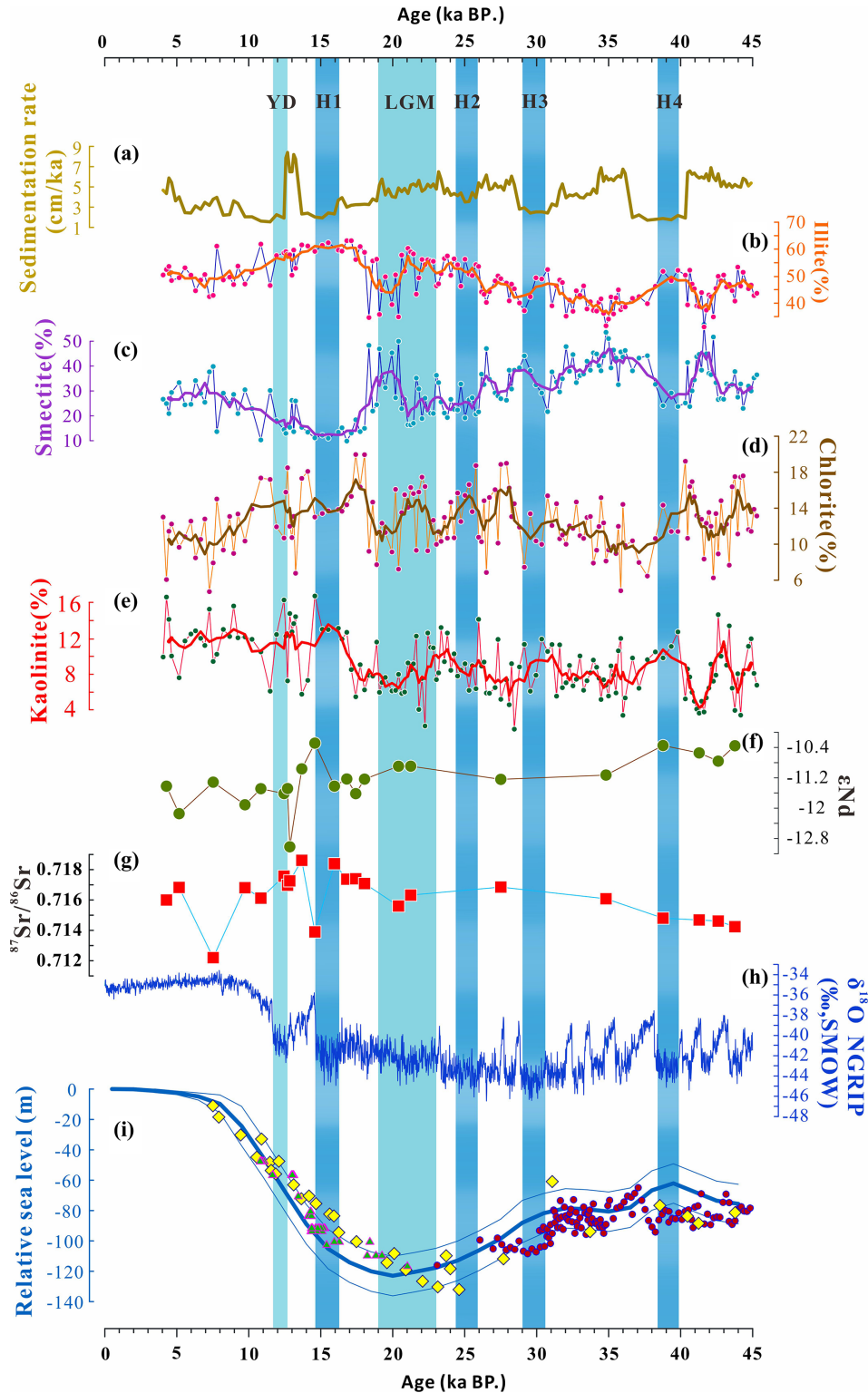


**Figure 3.** Comparison of clay mineral and Sr–Nd isotope data in the northeastern Indian Ocean with paleoclimate records. **(a)** Sedimentation rate in core 171106. **(b, c, d, e)** Illite, smectite, chlorite, and kaolinite percentages in core 171106 (thick line represents a three-point running average). **(f, g)**  $^{87}\text{Sr}/^{86}\text{Sr}$  and  $\epsilon\text{Nd}$  values of core 171106 in the northeastern Indian Ocean. **(h)**  $\delta^{18}\text{O}$  data from a Greenland ice core – NGRIP (Svensson et al., 2008). **(i)** Global sea level as a proxy for ice volume, reconstructed from benthic  $\delta^{18}\text{O}$  (thick cyan line; the thin cyan line represents the 95 % confidence interval; Thompson and Goldstein, 2006), globally distributed corals (yellow dots, Waelbroeck et al., 2002), and sea level data (triangles and red dots) collected by Grant et al. (2014) and Hanebuth et al. (2000). Blue and cyan bars represent cold-climate periods of Heinrich events (H1–H4) together with Younger Dryas (YD) and the Last Glacial Maximum (LGM), respectively.

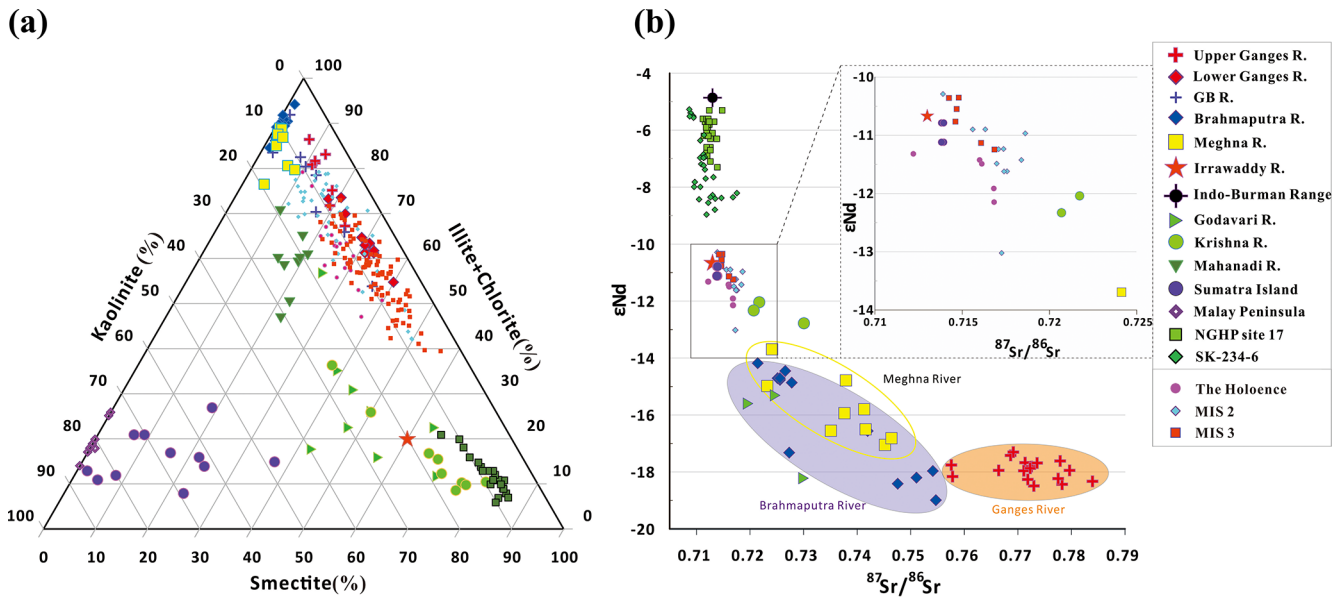


**Figure 4.** Sediment provenance of core 17I106 in the northeastern Indian Ocean. **(a)** Sediment provenance discrimination diagram in the northeastern Indian Ocean. For comparison, clay mineral data obtained from sediments collected in the modern Ganges River, Brahmaputra River lower, Ganges–Brahmaputra River lower and Meghna River (Khan et al., 2019), Mahanadi and Krishna rivers on the Indian Peninsula (Bejugam and Nayak, 2017), Irrawaddy River (Rodolfo, 1969), and Sumatra and Malay Peninsula rivers (Liu et al., 2012) are also plotted. The referenced cores comprise NGHP Site 17 (Ali et al., 2015), representing the Irrawaddy River as the main clay mineral source in the Andaman Sea. **(b)** Variations in  $\epsilon_{Nd}$  (0) vs.  $^{87}Sr/^{86}Sr$  measured in core 17I106 compared with those measured in river sediments and bulk rock samples collected around the BoB. In this diagram, we display data collected from Indian river samples (from the Godavari and Krishna rivers) (Ahmad et al., 2009) from different parts of the modern G-B River system (Lupker et al., 2013). Measurements taken from sediments obtained from the Irrawaddy River (Colin et al., 1999), formations from the Indo-Burman ranges (Licht et al., 2013), and volcanic products of Sumatra (Turner and Foden, 2001) are also plotted. The referenced cores include NGHP Sites 17 and SK-234-60, both of which indicate that the Irrawaddy River is the main Sr–Nd isotope source for the Andaman Sea.

surface current in the middle strait (MS) loads sediments of the Irrawaddy River southwest into the study area (Chatterjee et al., 2017).

#### 4.2 Factors affecting sediment provision

In general, illite is the major mineral produced during the strong physical erosion of metamorphic rocks and granite rocks as well as during the reprocessing of sedimentary rocks (Chamley, 1989; Winkler et al., 2002), while smectite is the secondary mineral produced during the chemical weathering of parent aluminosilicate and iron–magnesium silicate under warm and humid climate conditions (Chamley, 1989; Hillier, 1995). The climatic forces from the North Atlantic are thought to extensively impact the tropical eastern Indian Ocean (EIO) and surrounding areas of the BoB (Sun et al., 2011; DiNezio and Tierney, 2013; Dutt et al., 2015; Gautam et al., 2020; Mohtadi et al., 2014; Liu et al., 2021), whose climate signals can be transmitted via the tropical Atlantic bipolar surface sea temperature (SST) anomaly and associated southward shift of the ITCZ (Marzin et al., 2013), westerlies teleconnection and sea ice (Sun et al., 2011), or the reorganization of the Hadley circulation (Mohtadi et al., 2014).

During the North Atlantic cold-climate periods (Heinrich events and YD period, Fig. 3h), when rainfall and temperatures decreased in the South Asian monsoon region (An et al., 2011; DiNezio and Tierney, 2013; Gautam et al., 2020), physical weathering was enhanced in the Himalayas (Jousain et al., 2016), which made illite percentages at core 17I106 relatively high during these cold-climate periods, but chemical weathering weakened in Myanmar, and the smectite percentage thus decreased in the source area before these cold periods and continued to increase after these periods. The increasing (decreasing) trend of illite (smectite) percentages before cold-climate periods and the decreasing (increasing) trend of illite (smectite) percentages after cold-climate periods in our records suggest that the weathering degree in the source area influenced the supply of clay minerals during these cold-climate periods.

Sea level fluctuation is also critical in controlling the supplementation of terrestrial materials, especially clay minerals (Li et al., 2018; Liu et al., 2019), by changing the transport paths and/or distances as well as the further input of sediments into the study area. The changing trends of the sea level in seas adjacent to the BoB (Fig. 3i, Waelbroeck et al., 2002; Grant et al., 2014; Hanebuth et al., 2000; Thomp-

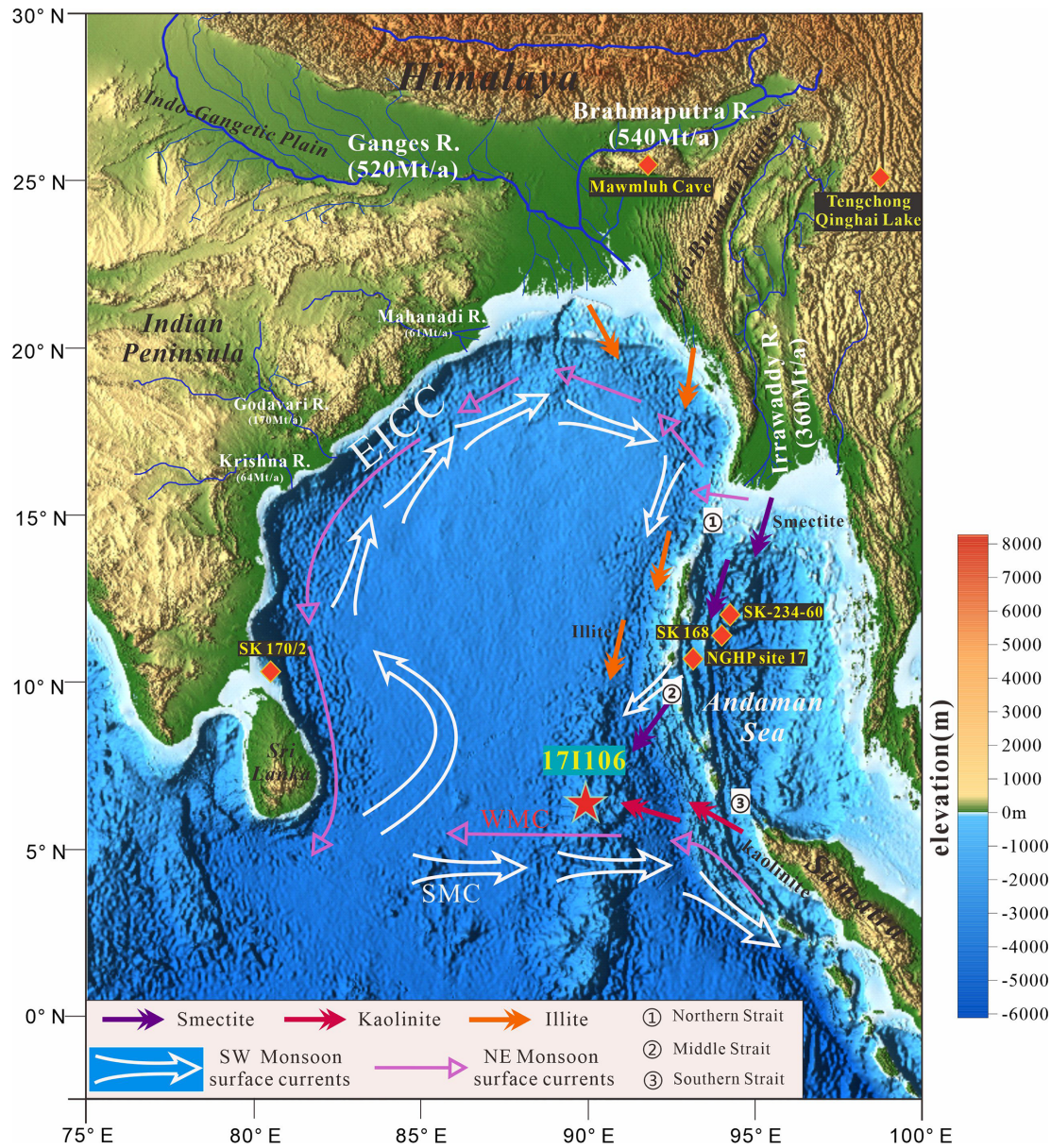


**Figure 5.** Map showing dispersal patterns of the BoB clay minerals for core 171106. The locations of core 171106 (red asterisks) and of the reference core and sites are shown: SK 170/2 in the northern BoB, SK-168, SK-234-60, NGHP Site 17 in the western Andaman Sea, Mawmluh Cave in northeastern India, and Tengchong Qinghai Lake in China are represented by orange diamonds. The orange, purple, and red arrows represent the main dispersal directions of illite, smectite, and kaolinite when the fluvial sediments were discharged into core 171106. The white and red arrows denote the SW and NE monsoon currents, respectively. In the western BoB, the East Indian Coastal Current (EICC) reverses annually with the monsoon wind (Schott and McCreary, 2001). In the lower-latitude regions of the BoB, monsoon-driven currents flow eastward in summer to form the summer monsoon current (SMC) and westward in winter to form the winter monsoon current (WMC) (Shankar et al., 2002). The elevation legend is shown to the right of this figure.

son and Goldstein, 2006) are well correlated with the smectite percentages measured in core 171106, especially during 35–21 ka, when the smectite percentages declined continuously. Since the Andaman and Nicobar Islands connecting the Andaman Sea and the BoB have continuously expanded as the sea level has continuously declined, the strait width has been consistently reduced, thereby preventing the entrance

of terrestrial materials into the Andaman Sea and the further continuous decline in smectite percentages in the study area. Here, we suggest that the variations in the measured illite percentages were mainly caused by changes in smectite deposition because the sedimentary records obtained from the northern BoB do not support the controlling effect of sea level on illite percentages over the past 50 kyr (Joussain et

al., 2016; Li et al., 2018; Liu et al., 2019). The relative exposure of 200 km from the current Irrawaddy River delta may affect the deposition process on the continental shelf or further deposition of the sediments delivered to the deep ocean, but core 17I106 is formed by the long-distance transport of large amounts of fine-grained terrestrial material, indicating that these sediments can be transported over long distances, and the  $\sim 200$  km change in the shelf distance is not a dominant factor of sediment transport in the study area. Moreover, the decreasing smectite percentages from the Myanmar area as sea level decreases suggest that shelf denudation is also not the main factor affecting our smectite record, which is in accordance with previous studies in the Andaman Sea that have not specifically emphasized the alteration of terrestrial source material supply by exposed shelves (Ali et al., 2015; Awasthi et al., 2014).

The South Asian summer monsoon is normally thought to be an important factor affecting weathering conditions around the BoB (Dutt et al., 2015; Gebregiorgis et al., 2016; Jousain et al., 2017; Li et al., 2018; Rashid et al., 2011; Zhang et al., 2020; Zorzi et al., 2015). Stalagmites in Mawmluh Cave record variations in river runoff in the surrounding area; these variations are determined by the impacts of surface sea temperature (SST) and water vapor transport paths (Dutt et al., 2015). In fact, the Mawmluh Cave records of the South Asian monsoon strength are driven by temperature gradients that drive changes in winds and moisture transport into the BoB (Dutt et al., 2015), not just responding to the rainfall amount. The smectite percentage changes measured in core 17I106 were slightly correlated after Heinrich event 1 (H1) but were irrelevant before H1 (Fig. 6b). This indicated that the combination of temperature and moisture failed to play a crucial role in smectite transport to core 17I106, although weathering features in the source area may be shaped by the South Asian monsoon. Moreover, the view could be confirmed by the smectite record obtained from the studied core not being well correlated with records previously obtained in the Andaman Sea (Fig. 6c, d, Gebregiorgis et al., 2016) or with a sporopollen record obtained in southwestern China (Fig. 6e, f, Zhang et al., 2020), especially before the LGM. The consistency of salinity and SST in core SK 168 (Fig. 6c, d) as well as moisture and temperature index (Fig. 6e, f) in southwestern China reveal that the hydroclimate in the South Asian monsoon region might have been influenced by SST in the Indian Ocean. All these inconsistencies between the smectite percentage in core 17I106 and monsoon records indicate that smectite supplementation may be mainly controlled by rainfall rather than by chemical weathering due to thermodynamic differences between sea and land environments (S. Liu et al., 2020).

During the late LGM, the smectite percentage increased abnormally in core 17I106, and this increase cannot be explained by dry and cold weathering conditions, a lower sea level, or a weakened summer monsoon at that time. In contrast, this abnormal change may have been attributed to an

increase in the smectite input in sediments from the Burman source area or to a decrease in the amounts of sediment input from the Himalayas. Under the influence of the winter monsoon during the LGM, the denuded sediments on the Irrawaddy estuary shelf may have been transported southward through the west side of Andaman Island (Prajith et al., 2018), as was confirmed in previous work showing that the winter monsoon led to an increase in terrestrial materials from the Irrawaddy River to the Ninetyeast Ridge during the Heinrich event (Ahmad et al., 2005). However, the winter monsoon was strong in the western part of the study area from 21 to 15 ka (Fig. 6g), and the sea level remained relatively low during that period (Gautam et al., 2020). The smectite percentages in the studied core increased significantly from 21 to 19 ka and dropped rapidly after 19 ka. This inconsistency contradicts the conclusion that the increased smectite percentage in the source area was caused by a strong winter monsoon. Moreover, the changes in the sediment compositions measured in the Himalayan source area were probably related to variations in regional glaciers. During the LGM period, the increased glacial cover may have reduced surface runoff and enhanced the transport of physical weathering products, while the increased amount of ice meltwater may have transported more illites following glacial melt. However, the reduced glacial area in the Himalayas during 18–15 ka did not occur simultaneously with the increased illite percentage (Yan et al., 2020; Weldeab et al., 2019, Fig. 6h). Therefore, the abnormal changes measured in the smectite percentage during the late LGM period were caused by other climate-driven mechanisms, and the millennium-scale smectite percentage fluctuations that occurred before the LGM require a more reasonable explanation.

#### 4.3 The ITCZ shift in the EIO

Changes in rainfall and the corresponding runoff are generally utilized to explain short-term variations in clay minerals. In the EIO, rainfall is controlled by monsoon activities (An et al., 2011; Beck et al., 2018; Gebregiorgis et al., 2016) and/or ITCZ migrations (Deplazes et al., 2013; Stoll et al., 2007; Tan et al., 2019). Glacial–interglacial monsoon precipitation changes at the regional scale are shaped by dynamics (changes in the wind fields) and temperature (McGee, 2020). The wind fields may be driven by the relative dominance of the northern low-pressure and southern high-pressure systems (An et al., 2011) as well as cross-equatorial moisture transport (Clemens et al., 2021), while the SST in the eastern Indian Ocean (Zhang et al., 2020) and western Indian Ocean (Wang et al., 2022), surface and subsurface temperature changes (Tierney et al., 2015), and temperature gradients (Weldeab et al., 2022) also play an important role in South Asian rainfall. At the same time, as a climate-driving force in low-latitude regions, ITCZ migrations may be the main factor responsible for regional hydrological changes (Deplazes

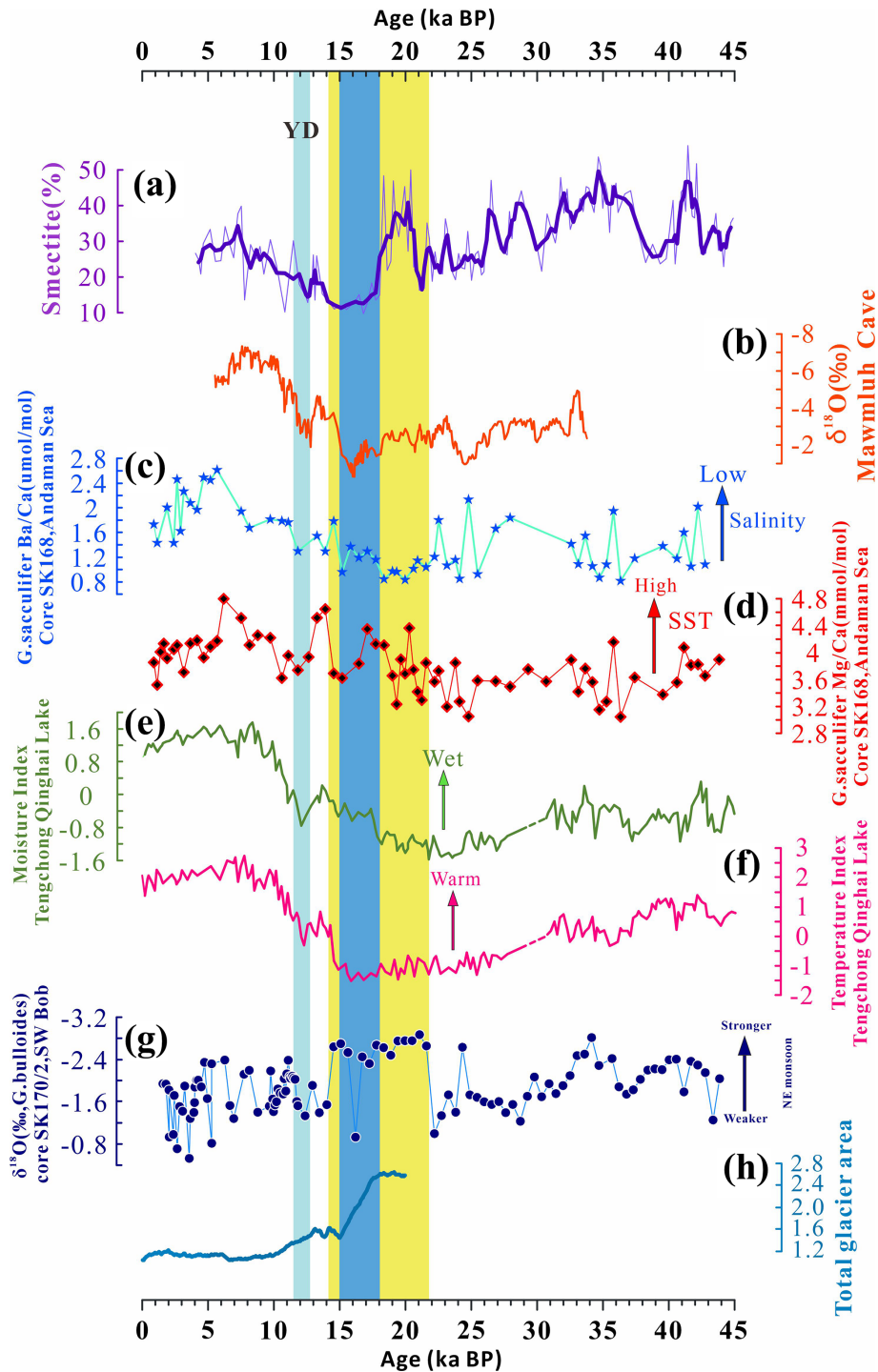


**Figure 6.** Comparison of smectite percentages in core 171106 with paleoclimate records. **(a)** Smectite percentages in core 171106 (thick line represents a 3-point running average); **(b)** Mawmluh Cave  $\delta^{18}\text{O}$  record for the interval 33 800 to 5500 years BP (Dutt et al., 2015). **(c, d)** Ba/Ca and Mg/Ca of the mixed layer species *G. sacculifer* in core SK 168 from the Andaman Sea, which represent the sea surface salinity and temperature; the lower salinity and higher temperature showed a strong SW monsoon (Gebregiorgis et al., 2016). **(e, f)** Moisture index and temperature index from pollen records from Tengchong Qinghai Lake (Peng et al., 2019; Zhang et al., 2020). **(g)**  $\delta^{18}\text{O}$  variability record of planktic foraminifera *Orbulina universa* obtained from core SK 170/2 recovered from the southwestern Bay of Bengal, which represents the strength of the NE monsoon (Gautam et al., 2020). **(h)** Ratio of the modeled total glacier area over the southern parts of the Himalayan–Tibetan orogen to the present level (Yan et al., 2020). Yellow, blue, and cyan bars represent the strong NE monsoon period shown in **(g)**, the main periods of glacier melting in the southern Himalayas shown in **(h)**, and the cold-climate periods of the Younger Dryas (YD).

et al., 2013; Weber et al., 2018) since the shift in the ITCZ was considered to control rainfall distribution and intensity in central India over geological timescales (Zorzi et al., 2015) and to cause summer temperature and moisture fluctuations in southwestern China during the last deglaciation (Zhang et al., 2019).

During the glacial–interglacial period, the ITCZ migrated north–south and balanced thermal differences by transferring atmospheric heat; this process represents an indispensable climate-regulating power on Earth (Broccoli et al., 2006; McGee et al., 2018; Schneider et al., 2014). In the Cariaco Basin and Arabian Sea (Fig. 7a–b), tropical rainfall is highly correlated with the North Atlantic climate, and sea ice variations in the North Atlantic affect the north–south shift of the ITCZ in low-latitude regions through atmospheric circulation and ocean processes (Deplazes et al., 2013). The smectite particles measured in core 17I106 mainly came from the Myanmar source area; in this area, rainfall is greatly affected by the seasonal shift of the ITCZ. Before the LGM, the smectite percentages in the study core were well matched with the ITCZ record in the Arabian Sea, where the supplementation of smectite percentages reached the peak when the ITCZ shifted significantly northward (Fig. 2b; Deplazes et al., 2013). During cold-climate events, when the ITCZ moved significantly southward, rainfall decreased, and the smectite percentages decreased correspondingly in the source area. Therefore, we suggest that these changes in the smectite percentages in the studied core are correlated with ITCZ migration and that rainfall is an important factor determining the smectite percentage from the source area of Myanmar on the millennial scale. If precipitation induced by wind and temperature of the South Asian monsoon has an intense impact on the source area, the source area monsoon indicators, for example, foraminifera, sporopollen, stalagmite (Fig. 6) and other indicators, would correspondingly change, but our record failed to catch these variations in monsoon indicators in the BoB. We suggest that every factor affecting precipitation induced by wind and temperature of the South Asian monsoon, as mentioned above, may have made it difficult to cause millennial-scale fluctuations similar to the ITCZ shift during the MIS3 period. The South Asian monsoon is indeed the result of combined factors that may contribute to the heterogeneity of monsoon rainfall in the BoB, which were also influenced by the north–south shift of the ITCZ. In core 17I106, the corresponding variations in the relatively high smectite percentages and the northward shift of the ITCZ indicate that the northward movement of the ITCZ is the most important factor influencing the incremental changes in river sediment load corresponding to the increased smectite percentages in the Myanmar region. Here we emphasize that the northward and southward ITCZ shifts bring about rainfall increases and decreases relative to other rainfall forces. The changes in clay minerals reflect changes in clay mineral supply in the source area, and it is these relative increases and decreases in rainfall that lead to

changes, which is a response to environmental changes. The sporopollen evidence suggested a cold and wet period during MIS3 in Yunnan, China (Zhang et al., 2020), which may have been caused by the frequent northward movement of the ITCZ during this period.

Although the changes in smectite percentages in the study area are associated with ITCZ shifts before the LGM, the ITCZ shift in the Indo-Pacific warm pool (IPWP) was more “regional” than those in the Arabian Sea and the Cariaco Basin (Deplazes et al., 2013). During the late LGM, when the ITCZ did not move extensively in the Arabian Sea, the ITCZ gradually shifted northward in the IPWP from 21 to 18 ka (Fig. 7d, Ayliffe et al., 2013). However, the smectite percentage increased significantly in the study area, and we have excluded the possibility that the winter monsoon or meltwater influenced these changes. Further comparisons with IPWP records reveal that the ITCZ changes agree well with the smectite percentage variations during the late LGM, indicating that the northern migration of the ITCZ induced high smectite percentages in core 17I106 (Fig. 7c, d). These results suggest that the clay minerals of core 17I106 are inextricably linked to ITCZ shifts on the millennial scale. In summary, our smectite record shows that before the LGM, the ITCZ was in a relatively southerly position in the Myanmar area, while during the late LGM, the northward movement of the ITCZ in the BoB led to increased rainfall in the Myanmar source area and an increased supply of smectite. At the same time, the ITCZ was not significantly shifted in the Arabian Sea region either pre-LGM or post-LGM, which is what the Arabian Sea record shows (Deplazes et al., 2013).

The smectite percentage in the studied core is different from the ITCZ records in some periods, such as the late LGM, revealing that regional changes in the ITCZ were significantly obvious and that the ITCZ is not a simple N–S displacement. This consistency may indicate that the regional extension of the north–south thermodynamic gradient in the EIO exceeded that in the Arabian Sea and that the north–south shift of the ITCZ caused the climate systems of the Northern and Southern Hemisphere to be more closely connected in the EIO during the late LGM (Huang et al., 2019; Zhuravleva et al., 2021). A recent study considered less northward migration of the summer ITCZ position in the western BoB than in the eastern BoB during Heinrich Stadials HS1 and HS5 (Ota et al., 2022), which indicated that regional ITCZ variations in the BoB may be very common. These factors may be correlated with observed variations in regional air–sea interactions, such as the exposure of the Sunda Shelf (DiNezio and Tierney, 2013), the effect of the thermocline in the EIO (Mohtadi et al., 2017), and even a potential El Niño-like mode (Thirumalai et al., 2019) and Indian Ocean dipole (IOD) (Abram et al., 2020) changes, which may make the ITCZ shift more dramatic or keep the ITCZ position in the Northern Hemisphere longer. Thus, the regional variations in the ITCZ should be fully considered when studying climate change, especially in low-

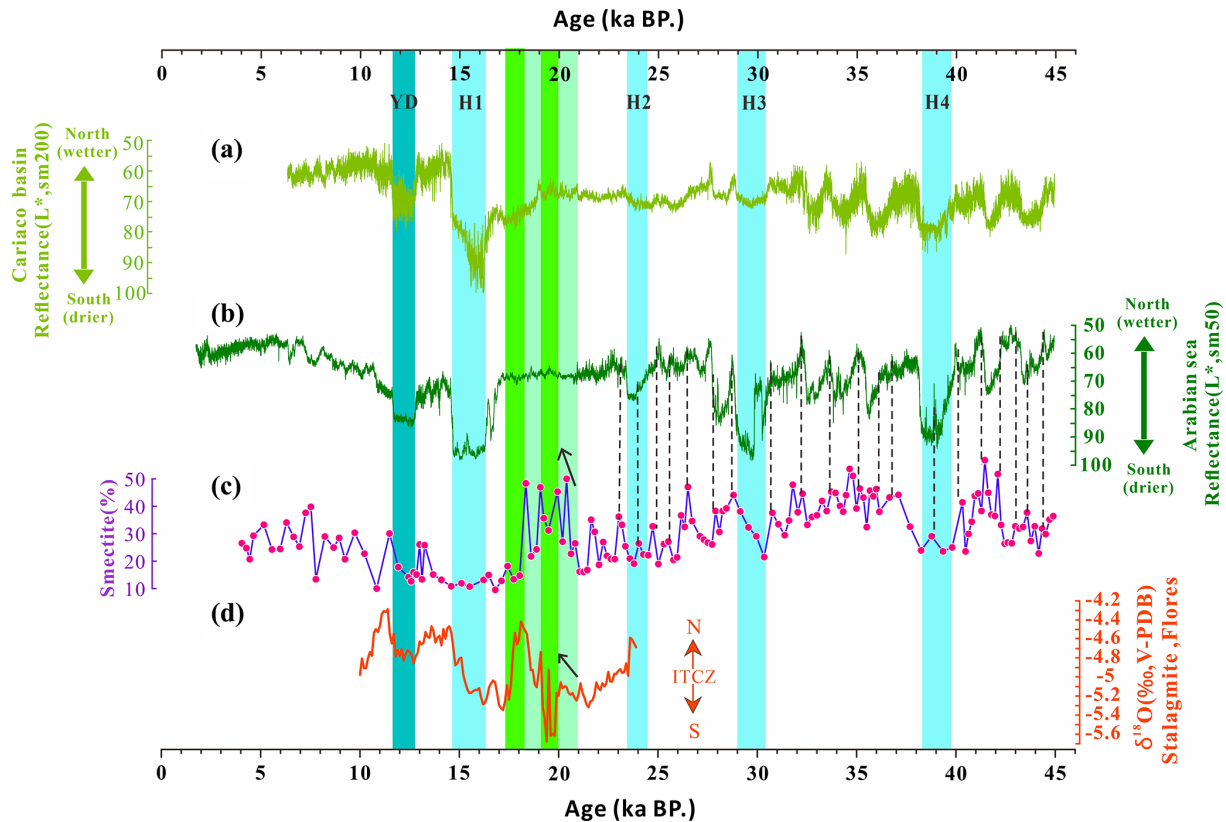


**Figure 7.** Comparison of smectite percentages with ITCZ north–south shift records. (a)  $L^*$  represents the ITCZ shift from the Cariaco Basin (Deplazes et al., 2013). (b)  $L^*$  represents the ITCZ shift from the Arabian Sea (Deplazes et al., 2013). (c) Smectite percentages in core 171106. (d) Stalagmite  $\delta^{18}\text{O}$  record from Flores (Ayliffe et al., 2013). The gold dotted line denotes the connection between the northward movement of the ITCZ and the peak smectite percentage, and the series of color bars from 21 to 18 ka represent the ITCZ shift periods recorded in (d). The green bars represent the consistent periods shown in (c, d) in the late LGM, and the black arrows in (c, d) indicate great differences between the smectite percentages and ITCZ record in the EIO.

latitude regions that are sensitive to climatic and environmental changes, such as the EIO (Niedermeyer et al., 2014).

## 5 Conclusion

We reconstructed the variations in sediment sources on the Ninetyeast Ridge over the past 45 kyr. The main source areas comprise the Himalayas transported by the G-B River and Irrawaddy River; sediments were stably supplied from these regions throughout the studied core. When North Atlantic cold events (Heinrich and YD) occurred, chemical weathering weakened and physical weathering increased; correspondingly, the smectite percentage decreased and the illite percentage increased. From 35 to 21 ka, the falling sea level led to an increase in the exposed area of the Andaman and Nicobar Islands and further hindered the entrance of smectite from the Andaman Sea into the study area. At the same time, the influence of the South Asian monsoon on the sediment supply was not obvious. The time-phase mismatches observed among records excluded the influence of Burman shelf sediment erosion forced by the winter monsoon or of

variations in G-B River sediments induced by ice meltwater on the abnormal increases observed in the smectite percentages during the late LGM. The smectite record of core 171106 is consistent with the ITCZ changes recorded on the millennial scale, indicating that the ITCZ controls the rainfall in the Burman source area and, further, the clay mineral variations in the study area. The inferred ITCZ shift recorded in the studied core coincided with the global ITCZ change that occurred before the LGM, but during the late LGM, the core record was consistent with the change in the regional ITCZ recorded by the IPWP. This revealed that regional changes in the ITCZ were very significant, and the ITCZ is not a simple N–S displacement at the same time. Thus, the regional variations in the ITCZ should be fully considered when studying climate change, especially in low-latitude regions that are sensitive to climate and environmental changes.

**Data availability.** The entire dataset is available on the Science Data Bank (<https://doi.org/10.11922/sciencedb.01188>; Xu et al., 2021).

**Author contributions.** JL and YH conceived and designed the experiment. XX wrote the paper with contributions from all authors. LZ and LY provided the ages of planktonic foraminifera, and SL, YY, LC, and LT helped to analyze the measured data and discuss the related relevant topics in this paper.

**Competing interests.** The contact author has declared that neither they nor their co-authors have any competing interests.

**Disclaimer.** Publisher's note: Copernicus Publications remains neutral with regard to jurisdictional claims in published maps and institutional affiliations.

**Acknowledgements.** We thank Hui Zhang for the help with Sr-Nd isotope measurements. We also thank the editor Pierre Francus, Michael E. Weber, and another anonymous reviewer for their constructive comments. Core sediment samples were collected on board the R/V *Shiyan 1* while implementing open research cruise NORC 2012-08 supported by the NSFC Shiptime Sharing Project.

**Financial support.** This research has been supported by the National Natural Science Foundation of China (grant nos. 42176075, 41576044, and 42130412), the Key Special Project for Introduced Talents Team of the Southern Marine Science and Engineering Guangdong Laboratory (Guangzhou) (grant no. GML2019ZD0206), the Bureau of Frontier Sciences and Education, Chinese Academy of Sciences (grant no. XDB42000000), and the Open Fund of the Key Laboratory of Submarine Geosciences, Ministry of Natural Resources (grant no. KLSG2102).

**Review statement.** This paper was edited by Pierre Francus and reviewed by Michael E. Weber and one anonymous referee.

## References

- Abram, N. J., Hargreaves, J. A., Wright, N. M., Thirumalai, K., Ummenhofer, C. C., and England, M. H.: Palaeoclimate perspectives on the Indian Ocean Dipole, *Quaternary Sci. Rev.*, 237, 106302, <https://doi.org/10.1016/j.quascirev.2020.106302>, 2020.
- Ahmad, S. M., Anil Babu, G., Padmakumari, V. M., Dayal, A. M., Sukhija, B. S., and Nagabhushanam, P.: Sr, Nd isotopic evidence of terrigenous flux variations in the Bay of Bengal: Implications of monsoons during the last ~ 34,000 years, *Geophys. Res. Lett.*, 32, L22711, <https://doi.org/10.1029/2005GL024519>, 2005.
- Ahmad, S. M., Padmakumari, V. M., and Babu, G. A.: Strontium and neodymium isotopic compositions in sediments from Godavari, Krishna and Pennar rivers, *Current Science*, 97, 1766–1769, 2009.
- Ali, S., Hathorne, E. C., Frank, M., Gebregiorgis, D., Stattegger, K., Stumpf, R., Kutterolf, S., Johnson, J. E., and Giosan, L.: South Asian monsoon history over the past 60 kyr recorded by radiogenic isotopes and clay mineral assemblages in the Andaman Sea, *Geochem. Geophys. Geos.*, 16, 505–521, <https://doi.org/10.1002/2014gc005586>, 2015.
- Ali, S., Hathorne, E. C., and Frank, M.: Persistent Provenance of South Asian Monsoon-Induced Silicate Weathering Over the Past 27 Million Years, *Paleoceanography and Paleoclimatology*, 36, e2020PA003909, <https://doi.org/10.1029/2020PA003909>, 2021.
- An, Z., Clemens, S., Shen, J., Qiang, X., Jin, Z., Sun, Y., Prell, W., Luo, J., Wang, S., Xu, H., Cai, Y., Zhou, W., Liu, X., Liu, W., Shi, Z., Yan, L., Xiao, X., Chang, H., Wu, F., Ai, L., and Lu, F.: Glacial-Interglacial Indian Summer Monsoon Dynamics, *Science*, 333, 719–723, <https://doi.org/10.1126/science.1203752>, 2011.
- Awasthi, N., Ray, J. S., Singh, A. K., Band, S. T., and Rai, V. K.: Provenance of the Late Quaternary sediments in the Andaman Sea: Implications for monsoon variability and ocean circulation, *Geochem. Geophys. Geos.*, 15, 3890–3906, <https://doi.org/10.1002/2014gc005462>, 2014.
- Ayliffe, L. K., Gagan, M. K., Zhao, J. X., Drysdale, R. N., Hellstrom, J. C., Hantoro, W. S., Griffiths, M. L., Scott-Gagan, H., Pierre, E. S., Cowley, J. A., and Suwargadi, B. W.: Rapid interhemispheric climate links via the Australasian monsoon during the last deglaciation, *Nat. Commun.*, 4, 2908, <https://doi.org/10.1038/ncomms3908>, 2013.
- Beck, J. W., Zhou, W., Li, C., Wu, Z., White, L., Xian, F., Kong, X. H., and An, Z.: A 550,000-year record of East Asian monsoon rainfall from Be-10 in loess, *Science*, 360, 877–881, <https://doi.org/10.1126/science.aam5825>, 2018.
- Bejugam, P. and Nayak, G. N.: Source and depositional processes of the surface sediments and their implications on productivity in recent past off Mahanadi to Pennar River mouths, western Bay of Bengal, *Palaeogeogr. Palaeoclimatol.*, 483, 58–69, <https://doi.org/10.1016/j.palaeo.2016.12.006>, 2017.
- Biscaye, P. E.: Mineralogy and sedimentation of recent deep-sea clay in Atlantic Ocean and adjacent seas and oceans, *Geol. Soc. Am. Bull.*, 76, 803–832, [https://doi.org/10.1130/0016-7606\(1965\)76\[803:masord\]2.0.co;2](https://doi.org/10.1130/0016-7606(1965)76[803:masord]2.0.co;2), 1965.
- Blaauw, M. and Christen, J. A.: Flexible Paleoclimate Age-Depth Models Using an Autoregressive Gamma Process, *Bayesian Anal.*, 6, 457–474, <https://doi.org/10.1214/11-ba618>, 2011.
- Broccoli, A. J., Dahl, K. A., and Stouffer, R. J.: Response of the ITCZ to Northern Hemisphere cooling, *Geophys. Res. Lett.*, 33, L01702, <https://doi.org/10.1029/2005GL024546>, 2006.
- Chamley, H.: *Clay Sedimentology*, Springer, Berlin, 623 pp., 1989.
- Chatterjee, A., Shankar, D., McCreary, J. P., Vinayachandran, P. N., and Mukherjee, A.: Dynamics of Andaman Sea circulation and its role in connecting the equatorial Indian Ocean to the Bay of Bengal, *J. Geophys. Res.-Oceans*, 122, 3200–3218, <https://doi.org/10.1002/2016JC012300>, 2017.
- Clemens, S. C., Yamamoto, M., Thirumalai, K., Giosan, L., Richey, J. N., Nilsson-Kerr, K., Rosenthal, Y., Anand, P., and McGrath, S. M.: Remote and local drivers of Pleistocene South Asian summer monsoon precipitation: A test for future predictions, *Sci. Adv.*, 7, eabg3848, <https://doi.org/10.1126/sciadv.abg3848>, 2021.
- Colin, C., Turpin, L., Bertaux, J., Desprairies, A., and Kissel, C.: Erosional history of the Himalayan and Burman Ranges during the last two glacial-interglacial cycles, *Earth Planet. Sc. Lett.*, 171, 647–660, [https://doi.org/10.1016/s0012-821x\(99\)00184-3](https://doi.org/10.1016/s0012-821x(99)00184-3), 1999.

- Colin, C., Turpin, L., Blamart, D., Frank, N., Kissel, C., and Duchamp, S.: Evolution of weathering patterns in the Indo-Burman Ranges over the last 280 kyr: Effects of sediment provenance on  $^{87}\text{Sr}/^{86}\text{Sr}$  ratios tracer, *Geochem. Geophys. Geosy.*, 7, Q03007, <https://doi.org/10.1029/2005gc000962>, 2006.
- Curray, J. R., Emmel, F. J., and Moore, D. G.: The Bengal Fan: morphology, geometry, stratigraphy, history and processes, *Mar. Petrol. Geol.*, 19, 1191–1223, [https://doi.org/10.1016/S0264-8172\(03\)00035-7](https://doi.org/10.1016/S0264-8172(03)00035-7), 2003.
- Deplazes, G., Lückge, A., Peterson, L. C., Timmermann, A., Hamann, Y., Hughen, K. A., Röhl, U., Laj, C., Cane, M. A., Sigman, D. M., and Haug, G. H.: Links between tropical rainfall and North Atlantic climate during the last glacial period, *Nat. Geosci.*, 6, 213–217, <https://doi.org/10.1038/ngeo1712>, 2013.
- DiNezio, P. N. and Tierney, J. E.: The effect of sea level on glacial Indo-Pacific climate, *Nat. Geosci.*, 6, 485–491, <https://doi.org/10.1038/ngeo1823>, 2013.
- Dou, Y., Yang, S., Shi, X., Clift, P. D., Liu, S., Liu, J., Li, C., Bi, L., and Zhao, Y.: Provenance weathering and erosion records in southern Okinawa Trough sediments since 28 ka: Geochemical and Sr–Nd–Pb isotopic evidences, *Chem. Geol.*, 425, 93–109, <https://doi.org/10.1016/j.chemgeo.2016.01.029>, 2016.
- Dutt, S., Gupta, A. K., Clemens, S. C., Cheng, H., Singh, R. K., Kathayat, G., and Edwards, R. L.: Abrupt changes in Indian summer monsoon strength during 33,800 to 5500 years B.P., *Geophys. Res. Lett.*, 42, 5526–5532, <https://doi.org/10.1002/2015gl064015>, 2015.
- Fournier, L., Fauquembergue, K., Zaragosi, S., Zorzi, C., Malaize, B., Bassinot, F., Joussain, R., Colin, C., Moreno, E., and Leparmentier, F.: The Bengal fan: external controls on the Holocene Active Channel turbidite activity, *Holocene*, 27, 900–913, <https://doi.org/10.1177/0959683616675938>, 2017.
- Gautam, P. K., Narayana, A. C., Kumar, P. K., Bhavani, P. G., Yadava, M. G., and Jull, A. J. T.: Indian monsoon variability during the last 46 kyr: isotopic records of planktic foraminifera from southwestern Bay of Bengal, *J. Quaternary Sci.*, 36, 138–151, <https://doi.org/10.1002/jqs.3263>, 2020.
- Gebregiorgis, D., Hathorne, E. C., Sijinkumar, A. V., Nath, B. N., Nürnberg, D., and Frank, M.: South Asian summer monsoon variability during the last ~54 kyrs inferred from surface water salinity and river runoff proxies, *Quaternary Sci. Rev.*, 138, 6–15, <https://doi.org/10.1016/j.quascirev.2016.02.012>, 2016.
- Gibbs, R. J.: Clay mineral segregation in the marine environment, *J. Sediment. Res.*, 47, 237–243, 1977.
- Goodbred, S. L. and Kuehl, S. A.: Enormous Ganges-Brahmaputra sediment discharge during strengthened early Holocene monsoon, *Geology*, 28, 1083–1086, [https://doi.org/10.1130/0091-7613\(2000\)028<1083:Egbsdd>2.3.Co;2](https://doi.org/10.1130/0091-7613(2000)028<1083:Egbsdd>2.3.Co;2), 2000.
- Grant, K. M., Rohling, E. J., Ramsey, C. B., Cheng, H., Edwards, R. L., Florindo, F., Heslop, D., Marra, F., Roberts, A. P., Tamisiea, M. E., and Williams, F.: Sea-level variability over five glacial cycles, *Nat. Commun.*, 5, 5076, <https://doi.org/10.1038/ncomms6076>, 2014.
- Hanebuth, T., Statterger, K., and Grootes, P. M.: Rapid Flooding of the Sunda Shelf: A Late-Glacial Sea-Level Record, *Science*, 288, 1033–1035, <https://doi.org/10.1126/science.288.5468.1033>, 2000.
- Hillier, S.: Erosion, Sedimentation and sedimentary origin of clays, in: *Origin and Mineralogy of Clays*. Clays Environment, edited by: Velde, B., Springer, Berlin, 162–219, [https://doi.org/10.1007/978-3-662-12648-6\\_4](https://doi.org/10.1007/978-3-662-12648-6_4), 1995.
- Huang, J., Wan, S., Li, A., and Li, T.: Two-phase structure of tropical hydroclimate during Heinrich Stadial 1 and its global implications, *Quaternary Sci. Rev.*, 222, 105900, <https://doi.org/10.1016/j.quascirev.2019.105900>, 2019.
- Jacobsen, S. B. and Wasserburg, G. J.: Sm–Nd isotopic evolution of chondrites, *Earth Planet. Sc. Lett.*, 50, 139–155, [https://doi.org/10.1016/0012-821x\(80\)90125-9](https://doi.org/10.1016/0012-821x(80)90125-9), 1980.
- Joussain, R., Colin, C., Liu, Z., Meynadier, L., Fournier, L., Fauquembergue, K., Zaragosi, S., Schmidt, F., Rojas, V., and Bassinot, F.: Climatic control of sediment transport from the Himalayas to the proximal NE Bengal Fan during the last glacial-interglacial cycle, *Quaternary Sci. Rev.*, 148, 1–16, <https://doi.org/10.1016/j.quascirev.2016.06.016>, 2016.
- Joussain, R., Liu, Z., Colin, C., Duchamp-Alphonse, S., Yu, Z., Moréno, E., Fournier, L., Zaragosi, S., Dapoigny, A., Meynadier, L., and Bassinot, F.: Link between Indian monsoon rainfall and physical erosion in the Himalayan system during the Holocene, *Geochem. Geophys. Geosy.*, 18, 3452–3469, <https://doi.org/10.1002/2016gc006762>, 2017.
- Kessarkar, P. M., Rao, V. P., Ahmad, S. M., Patil, S. K., Kumar, A. A., Babu, G. A., Chakraborty, S., and Rajan, R. S.: Changing sedimentary environment during the Late Quaternary: Sedimentological and isotopic evidence from the distal Bengal Fan, *Deep-Sea Res. Pt. I*, 52, 1591–1615, <https://doi.org/10.1016/j.dsr.2005.01.009>, 2005.
- Khan, M. H. R., Liu, J., Liu, S., Seddique, A. A., Cao, L., and Rahman, A.: Clay mineral compositions in surface sediments of the Ganges-Brahmaputra-Meghna river system of Bengal Basin, Bangladesh, *Mar. Geol.*, 412, 27–36, <https://doi.org/10.1016/j.margeo.2019.03.007>, 2019.
- Li, J., Liu, S., Shi, X., Feng, X., Fang, X., Cao, P., Sun, X.Q., Ye, W.X., Khokiattiwong, S., and Kornkanitnan, N.: Distributions of clay minerals in surface sediments of the middle Bay of Bengal: Source and transport pattern, *Contin. Shelf Res.*, 145, 59–67, <https://doi.org/10.1016/j.csr.2017.06.017>, 2017.
- Li, J., Liu, S., Shi, X., Zhang, H., Fang, X., Chen, M.-T., Cao, P., Sun, X. Q., Ye, W. X., Wu, K. K., Khokiattiwong, S., and Kornkanitnan, N.: Clay minerals and Sr–Nd isotopic composition of the Bay of Bengal sediments: Implications for sediment provenance and climate control since 40 ka, *Quatern. Int.*, 493, 50–58, <https://doi.org/10.1016/j.quaint.2018.06.044>, 2018.
- Licht, A., France-Lanord, C., Reisberg, L., Fontaine, C., Soe, A. N., and Jaeger, J. J.: A palaeo Tibet–Myanmar connection? Reconstructing the Late Eocene drainage system of central Myanmar using a multi-proxy approach, *J. Geol. Soc.*, 170, 929–939, <https://doi.org/10.1144/jgs2012-126>, 2013.
- Liu, J., He, W., Cao, L., Zhu, Z., Xiang, R., Li, T., Shi, X., and Liu, S.: Staged fine-grained sediment supply from the Himalayas to the Bengal Fan in response to climate change over the past 50,000 years, *Quaternary Sci. Rev.*, 212, 164–177, <https://doi.org/10.1016/j.quascirev.2019.04.008>, 2019.
- Liu, J. P., Kuehl, S. A., Pierce, A. C., Williams, J., Blair, N. E., Harris, C., Aung, D. W., and Aye, Y. Y.: Fate of Ayeyarwady and Thanlwin Rivers Sediments in the Andaman Sea and Bay of Bengal, *Mar. Geol.*, 423, 106137, <https://doi.org/10.1016/j.margeo.2020.106137>, 2020.

- Liu, S., Li, J., Zhang, H., Cao, P., Mi, B., Khokiattiwong, S., Kornkanitnan, N., and Shi, X.: Complex response of weathering intensity registered in the Andaman Sea sediments to the Indian Summer Monsoon over the last 40 kyr, *Mar. Geol.*, 426, 106206, <https://doi.org/10.1016/j.margeo.2020.106206>, 2020.
- Liu, S., Ye, W., Cao, P., Zhang, H., Chen, M.-T., Li, X., Li, J., Pan, H.-J., Khokiattiwong, S., Kornkanitnan, N., and Shi, X.: Paleoclimatic responses in the tropical Indian Ocean to regional monsoon and global climate change over the last 42 kyr, *Mar. Geol.*, 438, 106542, <https://doi.org/10.1016/j.margeo.2021.106542>, 2021.
- Liu, Z., Wang, H., Hantoro, W. S., Sathiamurthy, E., Colin, C., Zhao, Y., and Li, J.: Climatic and tectonic controls on chemical weathering in tropical Southeast Asia (Malay Peninsula, Borneo, and Sumatra), *Chem. Geol.*, 291, 1–12, <https://doi.org/10.1016/j.chemgeo.2011.11.015>, 2012.
- Lupker, M., France-Lanord, C., Galy, V., Lavé, J., and Kudrass, H.: Increasing chemical weathering in the Himalayan system since the Last Glacial Maximum, *Earth Planet. Sc. Lett.*, 365, 243–252, <https://doi.org/10.1016/j.epsl.2013.01.038>, 2013.
- Marzin, C., Kallel, N., Kageyama, M., Duplessy, J.-C., and Braconnot, P.: Glacial fluctuations of the Indian monsoon and their relationship with North Atlantic climate: new data and modelling experiments, *Clim. Past*, 9, 2135–2151, <https://doi.org/10.5194/cp-9-2135-2013>, 2013.
- McGee, D.: Glacial-Interglacial Precipitation Changes, *Annu. Rev. Mar. Sci.*, 12, 525–557, <https://doi.org/10.1146/annurev-marine-010419-010859>, 2020.
- McGee, D., Moreno-Chamarro, E., Green, B., Marshall, J., Galbraith, E., and Bradtmiller, L.: Hemispherically asymmetric trade wind changes as signatures of past ITCZ shifts, *Quaternary Sci. Rev.*, 180, 214–228, <https://doi.org/10.1016/j.quascirev.2017.11.020>, 2018.
- Mohtadi, M., Prange, M., Oppo, D. W., De Pol-Holz, R., Merkel, U., Zhang, X., Steinke, S., and Luckge, A.: North Atlantic forcing of tropical Indian Ocean climate, *Nature*, 509, 76–80, <https://doi.org/10.1038/nature13196>, 2014.
- Mohtadi, M., Prange, M., and Steinke, S.: Palaeoclimatic insights into forcing and response of monsoon rainfall, *Nature*, 533, 191–199, <https://doi.org/10.1038/nature17450>, 2016.
- Mohtadi, M., Prange, M., Schefuss, E., and Jennerjahn, T. C.: Late Holocene slowdown of the Indian Ocean Walker circulation, *Nat. Commun.*, 8, 1015, <https://doi.org/10.1038/s41467-017-00855-3>, 2017.
- Niedermeyer, E. M., Sessions, A. L., Feakins, S. J., and Mohtadi, M.: Hydroclimate of the western Indo-Pacific Warm Pool during the past 24,000 years, *P. Natl. Acad. Sci. USA*, 111, 9402–9406, <https://doi.org/10.1073/pnas.1323585111>, 2014.
- Ota, Y., Kawahata, H., Kuroda, J., Suzuki, A., Abe-Ouchi, A., and Jimenez-Espejo, F. J.: Millennial-scale variability of Indian summer monsoon constrained by the western Bay of Bengal sediments: Implication from geochemical proxies of sea surface salinity and river runoff, *Global Planet. Change*, 208, 103719, <https://doi.org/10.1016/j.gloplacha.2021.103719>, 2022.
- Peng, J., Yang, X., Toney, J.L., Ruan, J., Li, G., Zhou, Q., Gao, H., Xie, Y., Chen, Q., and Zhang, T.: Indian Summer Monsoon variations and competing influences between hemispheres since ~ 35 ka recorded in Tengchongqinghai Lake, southwestern China, *Palaeogeogr. Palaeoclimatol.*, 516, 113–125, <https://doi.org/10.1016/j.palaeo.2018.11.040>, 2019.
- Prajith, A., Tyagi, A., and John Kurian, P.: Changing sediment sources in the Bay of Bengal: Evidence of summer monsoon intensification and ice-melt over Himalaya during the Late Quaternary, *Palaeogeogr. Palaeoclimatol.*, 511, 309–318, <https://doi.org/10.1016/j.palaeo.2018.08.016>, 2018.
- Rashid, H., England, E., Thompson, L., and Polyak, L.: Late Glacial to Holocene Indian Summer Monsoon Variability Based upon Sediment Records Taken from the Bay of Bengal, *Terr. Atmos. Ocean. Sci.*, 22, 215–228, [https://doi.org/10.3319/TAO.2010.09.17.02\(TibXS\)](https://doi.org/10.3319/TAO.2010.09.17.02(TibXS)), 2011.
- Rayaroth, M. K., Peter, B. N., and Mahmud, M. R.: High-resolution surface circulation of the Bay of Bengal derived from satellite observation data, *J. Mar. Sci. Technol.*, 24, 656–668, <https://doi.org/10.6119/JMST-015-1215-2>, 2016.
- Raza, T. and Ahmad, S. M.: Surface and deep water variations in the northeast Indian Ocean during 34–6 ka BP: evidence from carbon and oxygen isotopes of fossil foraminifera, *Quatern. Int.*, 298, 37–44, <https://doi.org/10.1016/j.quaint.2012.05.005>, 2013.
- Reimer, P. J., Austin, W. E. N., Bard, E., Bayliss, A., Blackwell, P. G., Bronk Ramsey, C., Butzin, M., Cheng, H., Edwards, R. L., Friedrich, M., Grootes, P. M., Guilderson, T. P., Hajdas, I., Heaton, T. J., Hogg, A. G., Hughen, K. A., Kromer, B., Manning, S. W., Muscheler, R., Palmer, J. G., Pearson, C., van der Plicht, J., Reimer, R. W., Richards, D. A., Scott, E. M., Southon, J. R., Turney, C. S. M., Wacker, L., Adolphi, F., Büntgen, U., Capano, M., Fahrni, S. M., Fogtmann-Schulz, A., Friedrich, R., Köhler, P., Kudsk, S., Miyake, F., Olsen, J., Reinig, F., Sakamoto, M., Sookdeo, A., and Talamo, S.: The intcal20 northern hemisphere radiocarbon age calibration curve (0–55 cal kBP), *Radiocarbon*, 62, 725–757, <https://doi.org/10.1017/RDC.2020.41>, 2020.
- Rodolfo, K. S.: Sediments of Andaman Basin, northeastern Indian Ocean, *Mar. Geol.*, 7, 371–380, [https://doi.org/10.1016/0025-3227\(69\)90014-0](https://doi.org/10.1016/0025-3227(69)90014-0), 1969.
- Schneider, T., Bischoff, T., and Haug, G. H.: Migrations and dynamics of the intertropical convergence zone, *Nature*, 513, 45–53, <https://doi.org/10.1038/nature13636>, 2014.
- Schott, F. A. and McCreary, J. P.: The monsoon circulation of the Indian Ocean, *Prog. Oceanogr.*, 51, 1–123, [https://doi.org/10.1016/s0079-6611\(01\)00083-0](https://doi.org/10.1016/s0079-6611(01)00083-0), 2001.
- Seo, I., Khim, B.-K., Cho, H.G., Huh, Y., Lee, J., and Hyeong, K.: Origin of the Holocene Sediments in the Ninetyeast Ridge of the Equatorial Indian Ocean, *Ocean Sci. J.*, <https://doi.org/10.1007/s12601-021-00052-w>, 2022.
- Shankar, D., Vinayachandran, P. N., and Unnikrishnan, A. S.: The monsoon currents in the north Indian Ocean, *Prog. Oceanogr.*, 52, 63–120, [https://doi.org/10.1016/s0079-6611\(02\)00024-1](https://doi.org/10.1016/s0079-6611(02)00024-1), 2002.
- Stoll, H. M., Vance, D., and Arevalos, A.: Records of the Nd isotope composition of seawater from the Bay of Bengal: Implications for the impact of Northern Hemisphere cooling on ITCZ movement, *Earth Planet. Sc. Lett.*, 255, 213–228, <https://doi.org/10.1016/j.epsl.2006.12.016>, 2007.
- Sun, Y., Clemens, S. C., Morrill, C., Lin, X., Wang, X., and An, Z.: Influence of Atlantic meridional overturning circulation on the East Asian winter monsoon, *Nat. Geosci.*, 5, 46–49, <https://doi.org/10.1038/ngeo1326>, 2011.

- Svensson, A., Andersen, K. K., Bigler, M., Clausen, H. B., Dahl-Jensen, D., Davies, S. M., Johnsen, S. J., Muscheler, R., Parrenin, F., Rasmussen, S. O., Röthlisberger, R., Seierstad, I., Steffensen, J. P., and Vinther, B. M.: A 60 000 year Greenland stratigraphic ice core chronology, *Clim. Past*, 4, 47–57, <https://doi.org/10.5194/cp-4-47-2008>, 2008.
- Tan, L., Shen, C. C., Lowemark, L., Chawchai, S., Edwards, R. L., Cai, Y., Breitenbach, S. F. M., Cheng, H., Chou, Y. C., Duerrast, H., Partin, J. W., Cai, W., Chabangborn, A., Gao, Y., Kwecien, O., Wu, C. C., Shi, Z., Hsu, H. H., and Wohlfarth, B.: Rainfall variations in central Indo-Pacific over the past 2,700 y, *P. Natl. Acad. Sci. USA*, 116, 17201–17206, <https://doi.org/10.1073/pnas.1903167116>, 2019.
- Thompson, W. G. and Goldstein, S. L.: A radiometric calibration of the SPECMAP timescale, *Quaternary Sci. Rev.*, 25, 3207–3215, <https://doi.org/10.1016/j.quascirev.2006.02.007>, 2006.
- Thirumalai, K., DiNezio, P. N., Tierney, J. E., Puy, M., and Mohtadi, M.: An El Niño Mode in the Glacial Indian Ocean?, *Paleoceanogr. Paleocl.*, 34, 1316–1327, <https://doi.org/10.1029/2019pa003669>, 2019.
- Tierney, J. E., Pausata, F. S. R., and deMenocal, P.: Deglacial Indian monsoon failure and North Atlantic stadials linked by Indian Ocean surface cooling, *Nat. Geosci.*, 9, 46–50, <https://doi.org/10.1038/ngeo2603>, 2015.
- Tripathy, G. R., Singh, S. K., and Bhushan, R.: Sr-Nd isotope composition of the Bay of Bengal sediment: Impact of climate on erosion in the Himalaya, *Geochem. J.*, 45, 175–186, 2011.
- Tripathy, G. R., Singh, S. K., and Ramaswamy, V.: Major and trace element geochemistry of Bay of Bengal sediments: Implications to provenances and their controlling factors, *Palaeogeogr., Palaeocl.*, 397, 20–30, <https://doi.org/10.1016/j.palaeo.2013.04.012>, 2014.
- Turner, S. and Foden, J.: U, Th and Ra disequilibria, Sr, Nd and Pb isotope and trace element variations in Sunda arc lavas: predominance of a subducted sediment component, *Contrib. Mineral. Petr.*, 142, 43–57, <https://doi.org/10.1007/s004100100271>, 2001.
- Waelbroeck, C., Labeyrie, L., Michela, E., Duplessy, J. C., McManus, J. F., Lambeck, K., Balbona, E., and Labracherie, M.: Sea-level and deep water temperature changes derived from benthic foraminifera isotopic records, *Quaternary Sci. Rev.*, 21, 295–305, [https://doi.org/10.1016/s0277-3791\(01\)00101-9](https://doi.org/10.1016/s0277-3791(01)00101-9), 2002.
- Wang, Y. V., Larsen, T., Lauterbach, S., Andersen, N., Blanz, T., Krebs-Kanzow, Gierz, P., and Schneider, R. R.: Higher sea surface temperature in the Indian Ocean during the Last Interglacial weakened the South Asian monsoon, *P. Natl. Acad. Sci. USA*, 119, e2107720119, <https://doi.org/10.1073/pnas.2107720119>, 2022.
- Weber, M. E., Lantzsich, H., Dekens, P., Das, S. K., Reilly, B. T., Martos, Y. M., Meyer-Jacob, C., Agrahari, S., Ekblad, A., Titschack, J., Holmes, B., and Wolfgramm, P.: 200,000 years of monsoonal history recorded on the lower Bengal Fan – strong response to insolation forcing, *Global Planet. Change*, 166, 107–119, <https://doi.org/10.1016/j.gloplacha.2018.04.003>, 2018.
- Weldeab, S., Rühlemann, C., Bookhagen, B., Pausata, F. S. R., and Perez-Lua, F. M.: Enhanced Himalayan Glacial Melting During YD and H1 Recorded in the Northern Bay of Bengal, *Geochem. Geophys. Geos.*, 20, 2449–2461, <https://doi.org/10.1029/2018GC008065>, 2019.
- Weldeab, S., Rühlemann, C., Ding, Q., Khon, V., Schneider, B., and Gray, W. R.: Impact of Indian Ocean surface temperature gradient reversals on the Indian Summer Monsoon, *Earth Planet. Sc. Lett.*, 578, 117327, <https://doi.org/10.1016/j.epsl.2021.117327>, 2022.
- Winkler, A., Wolf-Welling, T., Stattegger, K., and Thiede, J.: Clay mineral sedimentation in high northern latitude deep-sea basins since the Middle Miocene (ODP Leg 151, NAAG), *Int. J. Earth Sci.*, 91, 133–148, <https://doi.org/10.1007/s005310100199>, 2002.
- Xu, X., Liu, J., Huang, Y., Tan, L., and Cao, L.: Northeast Indian Ocean Marine Sediment core 17I106, Science Data Bank [data set], <https://doi.org/10.11922/sciencedb.01188>, 2021.
- Yan, Q., Owen, L. A., Zhang, Z., Jiang, N., and Zhang, R.: Deciphering the evolution and forcing mechanisms of glaciation over the Himalayan-Tibetan orogen during the past 20,000 years, *Earth Planet. Sc. Lett.*, 541, 116295, <https://doi.org/10.1016/j.epsl.2020.116295>, 2020.
- Ye, W., Liu, S., Fan, D., Zhang, H., Cao, P., Pan, H.-J., Li, J., Li, X., Fang, X., Khokiattiwong, S., Kornkanitnan, N., and Shi, X.: Evolution of sediment provenances and transport processes in the central Bay of Bengal since the Last Glacial Maximum, *Quatern. Int.*, <https://doi.org/10.1016/j.quaint.2020.12.007>, in press, 2020.
- Yu, Z., Colin, C., Wan, S., Saraswat, R., Song, L., Xu, Z., Clift, P., Lu, H., Lyle, M., Kulhanek, D., Hahn, A., Tiwari, M., Mishra, R., Miska, S., and Kumar, A.: Sea level-controlled sediment transport to the eastern Arabian Sea over the past 600 kyr: clay minerals and Sr-Nd isotopic evidence from IOD site U1457, *Quaternary Sci. Rev.*, 205, 22–34, <https://doi.org/10.1016/j.quascirev.2018.12.006>, 2019.
- Zhang, E., Chang, J., Shulmeister, J., Langdon, P., Sun, W., Cao, Y., Yang, X., and Shen, J.: Summer temperature fluctuations in Southwestern China during the end of the LGM and the last deglaciation, *Earth Planet. Sc. Lett.*, 509, 78–87, <https://doi.org/10.1016/j.epsl.2018.12.024>, 2019.
- Zhang, X., Zheng, Z., Huang, K., Yang, X., and Tian, L.: Sensitivity of altitudinal vegetation in southwest China to changes in the Indian summer monsoon during the past 68000 years, *Quaternary Sci. Rev.*, 239, 106359, <https://doi.org/10.1016/j.quascirev.2020.106359>, 2020.
- Zhuravleva, A., Hüls, M., Tiedemann, R., and Bauch, H. A.: A 125-ka record of northern South American precipitation and the role of high-to-low latitude teleconnections, *Quaternary Sci. Rev.*, 270, 107159, <https://doi.org/10.1016/j.quascirev.2021.107159>, 2021.
- Zorzi, C., Sanchez Goñi, M. F., Anupama, K., Prasad, S., Hanquiez, V., Johnson, J., and Giosan, L.: Indian monsoon variations during three contrasting climatic periods: The Holocene, Heinrich Stadial 2 and the last interglacial–glacial transition, *Quaternary Sci. Rev.*, 125, 50–60, <https://doi.org/10.1016/j.quascirev.2015.06.009>, 2015.